Scientific Research Publishing

Positioning, 2026, 17(1), 1-11
https://www.scirp.org/journal/pos
ISSN Online: 2150-8526
ISSN Print: 2150-850X

GPS Transmissivity through Light Rain

Mark D. Jacobson

Department of Mathematics, Montana State University Billings, Billings, MT, USA
Email: mjacobson@msubillings.edu

How to cite this paper: Jacobson, M.D. (2026) GPS Transmissivity through Light Rain. *Positioning*, **17**, 1-11.
https://doi.org/10.4236/pos.2026.171001

Received: November 25, 2025
Accepted: January 1, 2026
Published: January 4, 2026

Abstract

The Global Positioning System (GPS) is designed to operate in all weather conditions. Here, we discuss a case that involves received GPS signals through a light rain event, with incident energy at 1.57542 GHz right-hand circularly polarized. The power transmission of GPS signals to the receiver is referred to as GPS Transmissivity (GPS-T). The relative received powers through the light rain are measured with an antenna that is covered by a fiberglass hemispherical radome. The average rain rate is measured by a tipping-bucket-type rain gauge. This *in situ* measurement is used for calculating the approximate uniform water-layer thickness formed on the radome. The power transmission losses through the radome and water-layer thickness combination, the radome thickness alone, and the water-layer thickness alone are computed from conventional theory. The radome's power transmission loss is eliminated by subtracting the received power during the light rain from the received maximum power during the mostly clear skies. The measured maximum power transmission loss by the light rain for GPS satellite PRN 29 is approximately 2.5 decibels (dB). This translates to a minimum transmissivity of approximately 58%. The impact of these results is discussed.

Keywords

Global Positioning System, Power Transmission, Transmissivity, Power Transmission Loss, Light Rain, Radome

1. Introduction

The Global Positioning System (GPS) is designed to provide continuous positioning and timing information anywhere in the world under all weather conditions [1] [2]. This includes conditions when GPS signals propagate through rain. The power transmission loss of GPS signals by rain is degraded by both depolarization and attenuation. The power transmission of GPS signals to the receiver is referred to as GPS Transmissivity (GPS-T). This technique is slightly different than the

Global Navigation Satellite Systems Transmissiometry (GNSS-T) technique [3]. The primary difference between the two techniques is that GPS-T uses only one receiver, whereas GNSS-T uses two receivers. The GNSS-T technique requires that the two GNSS receivers be identical to measure the difference between the two signal strengths [3]. Therefore, the antenna gains and the front-end radio frequency circuitry must be identical for the two GNSS receivers. This is a potential limitation for this technique since these two receivers may not be identical. On the other hand, the GPS-T technique does not have this requirement since it uses only one GPS receiver. However, this technique requires that the transmitted satellite signal strength remains constant during the measurements so that the difference between the rain signal strength and the mostly clear skies signal strength can be calculated correctly. This is a potential limitation for this technique since variations in satellite transmission power could influence the calculated power loss. In this paper, GPS-T is measured for light rain (rain rate < 2.5 mm h^{-1} [4]).

Kobayashi [5] [6] showed that 4 GHz circularly polarized signals through rain are degraded much more by depolarization than by attenuation. For L-band frequencies, the rain attenuation is less than 0.1 dB km^{-1} for a rain rate of 150 mm h^{-1} [7] [8]. This is further validated by the absorption (attenuation) model for the GPS L1 frequency by [9] that indicates greater than 96% transmissivity (double-path integrated propagation loss of 0.07 dB) (depolarization is not included) for rain rates up to 30 mm h^{-1} and an integration height of approximately 4800 m. This translates to single-path integrated propagation losses of 0.035, 0.0035, and 0.0005 dB for rain rates of 30 mm h^{-1}, 2.5 mm h^{-1}, and 0.75 mm h^{-1}, respectively [9]. Therefore, rain attenuation is typically neglected at GNSS frequencies for rain rates up to 30 mm h^{-1}. However, the GPS-T measurements presented here include both rain depolarization and rain attenuation. Some rain effects on GNSS-R measurements over the ocean have recently been reported [9]-[12]. In contrast to these GNSS-R measurements over the ocean, the rain effects presented here are for GPS-T measurements over land. Furthermore, the GPS-T measurements are through the rain rather than the reflected signals from the ocean through the rain. The goal of the GPS-T measurements in this paper is to better understand and quantify how light rain affects GPS signals over land.

2. Wet Radome Considerations

A 61-cm-diameter, 3-mm-thick fiberglass hemispherical radome was leveled and centered over a horizontally mounted right-hand circularly polarized GPS antenna (see Section 3) to keep it dry during rain. **Figure 1** shows a photograph of the radome used in the measurements. The 30.50-cm radius (r) of the radome satisfies the far-field criteria of the antenna [13] since $r > 1.6 \times \lambda_0 = 30.45$ cm, where $\lambda_0 = 19.02937$ cm is the GPS L1 free-space wavelength. The value 1.6 is used because the maximum dimension of the GPS antenna, 2.0 cm < $\lambda_0/3 = 6.3$ cm. At 1.6 GHz, the approximate real relative permittivity of fiberglass is $\epsilon_r = 4.47$, and the approximate loss tangent ($\tan\delta$) is $\tan\delta \times 10^4 = 264$ [14].

Figure 1. The fiberglass hemispherical radome is leveled and centered over the GPS antenna.

Gibble's equation [15]-[18] is used to calculate the approximate uniform water-layer thickness (w) formed on the fiberglass hemispherical radome during rain. The fiberglass material enhances the laminar flow, which is necessary for this model. Gibble's equation is

$$w = \sqrt[3]{3\mu_s r R (2g)^{-1}} \tag{1}$$

where $\mu_s = 10^{-6}$ m^2 s^{-1} is the specific viscosity of water, $g = 10^{-6}$ m s^{-1} is the gravitational acceleration, R is the rain rate in m s^{-1}, and $r = 0.305$ m is the radius of the radome.

The complex relative permittivity value of pure liquid water at a temperature of 10.8˚C is computed [19] [20] as $\epsilon_w = 82.50 - i9.44$, where $i = \sqrt{-1}$.

To obtain an estimate of the power transmission (transmissivity) through the wet hemispherical radome, we deal with the simplest possible model: a plane wave normally incident upon a planar radome and adjacent uniform water layer where the radome does not absorb water. Therefore, a transmission line equivalent circuit for the two uniform layers is used to calculate the power transmission. The propagation constants and characteristic impedances of the different media are defined in [21].

$$\gamma = i2\pi f \sqrt{u_0 (\epsilon' - i\epsilon'')}, \text{ propagation constant (m}^{-1}) \tag{2}$$

$$Z = \sqrt{u_0 (\epsilon' - i\epsilon'')^{-1}}, \text{ characteristic impedance } (\Omega) \tag{3}$$

where $f = 1.57542 \times 10^9$ Hz; $\mu_0 = 4\pi \times 10^{-7}$ H m^{-1} (free-space permeability); $\epsilon' = \epsilon_r \left(\mu_0 c^2\right)^{-1} = \epsilon_r \epsilon_0$ (F m^{-1}) where ϵ_r is the real relative permittivity, $c = 2.997925 \times 10^8$ m s^{-1} (speed of light in a vacuum), and ϵ_0 is the free-space permittivity; and $\epsilon'' = \epsilon' \tan\delta$ (F m^{-1}) where $\tan\delta$ is the loss tangent (dimensionless).

To facilitate the use of the transmission line analogy for the radome and water-layer thicknesses, an equivalent two-port network using the ABCD matrix [21] [22] is shown to be

$$\begin{bmatrix} A & B \\ C & D \end{bmatrix} = \begin{bmatrix} C_1 & Z_1 S_1 \\ S_1 / Z_1 & C_1 \end{bmatrix} \begin{bmatrix} C_2 & Z_2 S_2 \\ S_2 / Z_2 & C_2 \end{bmatrix} \tag{4}$$

where

$$C_j = \cosh\left(\gamma_j d_j\right)$$

$$S_j = \sinh\left(\gamma_j d_j\right)$$

$$Z_j = \text{impedance of medium } j\left(\Omega\right)$$

$$d_j = \text{medium } j \text{ thickness}\left(m\right)$$

$$\gamma_j = \text{propagation constant in medium } j\left(m^{-1}\right)$$

for $j = 1$ for radome thickness; $j = 2$ for water-layer thickness.

To obtain the amplitude transmission (t), we convert the overall ABCD matrix (4) to a scattering matrix. For a reciprocal network, this gives [21]

$$t = 2Z_0 / G \tag{5}$$

where $Z_0 = \mu_0 c$, free-space impedance (Ω); $G = AZ_0 + B + CZ_0^2 + DZ_0$.

The power transmission (transmissivity) (T) is

$$T = |t|^2 \tag{6}$$

The power transmission loss (TL) in decibels (dB) is

$$TL = -10 \log_{10} T \tag{7}$$

3. Measurements during Light Rain

On June 2, 2025, from 6:21 p.m. to 6:48 p.m. Greenwich Mean Time (GMT), a Trimble Lassen LP GPS L1 (1.57542 GHz right-hand circularly polarized antenna) receiver was used to measure the GPS signals through light rain. The site for these measurements was located approximately 8 km west of Billings Logan International Airport, Billings, Montana. The antenna was magnetically attached to a 10 cm × 10 cm × 1.6 mm metal plate, which was taped to a 20 cm × 10 cm × 5 cm horizontally flat cement brick. The active Trimble antenna consists of a microstrip patch antenna (20 mm × 20 mm × 1.6 mm), a preamplifier, a radome, and a ground plane.

As stated in Section 2, a fiberglass hemispherical radome was leveled and centered over a horizontally mounted GPS antenna to keep it dry during rain (see **Figure 1**). Received GPS azimuth angles (AZ) were restricted to $180° \le AZ \le 360°$ for minimizing blockage and shadowing at the site, where $AZ = 360°$ is True North. In addition, received GPS elevation angles (EL) were restricted to $65° \le EL \le 90°$ for providing constant antenna gain, where $EL = 90°$ is Zenith. Satellite PRN 29 was chosen among the available GPS satellites of the constellation for these measurements because it had the only orbital track that met the azimuth and elevation angle criteria. The other available GPS satellites did not satisfy the elevation angle criterion, *i.e.*, the constant antenna gain criterion was not met. This criterion is critical to ensure that the received signals during the measurements are not de-

graded by the antenna gain. This is one limitation of this technique. The second limitation of this technique is that it assumes that the transmitted satellite signal strength was constant during the measurements. This is a potential limitation since variations in satellite transmission power could influence the calculated power loss. During this time, GPS satellite PRN 29's azimuth angles decreased from 307.7° to 304.3°, and its elevation angles increased from 65.0° to 77.5°. Signal power levels were collected for approximately 27 minutes to characterize the power transmission properties through the light rain. Power levels (P_{dB}) were directly recorded in dB from the GPS receiver every 0.5 s to a laptop computer.

The rain rate at the site was measured by a tipping-bucket-type rain gauge (RainWise). The rain gauge was located 8.5 m from the GPS antenna at a height of 1 m above the ground. The bucket records a signal for every 0.1 mm/tip. During the light rain event, the rain gauge produced 3 signals at 6:29 p.m., 6:34 p.m., and 6:42 p.m. GMT. Visually, the rain rate was less from 6:21 p.m. to 6:25 p.m. GMT. Then the rain rate increased from 6:25 p.m. to 6:45 p.m. GMT. The rain stopped at 6:45 p.m. GMT. The skies became mostly clear from 6:45 p.m. to 6:48 p.m. GMT. During this time, the radome surface was dry. From 6:21 p.m. to 6:45 p.m. GMT, the average rain rate was calculated to be 0.75 mm h^{-1}. This is considered light rain since the rain rate result is less than 2.5 mm h^{-1} [4]. The average air temperature was 10.8˚C during this time.

From (1), a rain rate of 0.75 mm h^{-1} produces a water-layer thickness (w) of 0.021 mm. Therefore, the calculated power transmission losses through the radome and water-layer thickness combination, the radome thickness alone, and the water-layer thickness alone are 0.26, 0.17, and 0.05 dB, respectively, from (7). The real relative permittivity and loss tangent of the fiberglass, and the complex relative permittivity of the water (see Section 2) are used in the above calculations.

The measured power transmission loss (TL) through the light rain event is estimated as

$$TL = P_{\max dB} - P_{dB} \tag{8}$$

where

TL: power transmission loss in dB;

P_{dB}: received power in dB;

P_{masdB}: received maximum power in dB during the mostly clear skies.

The subtraction process in (8) eliminates the radome's power transmission loss of 0.17 dB (see Section 2). Furthermore, the water-layer's power transmission loss on the radome of 0.05 dB (see Section 2) is neglected because it is much less than the measured power transmission losses during the light rain (see **Figure 2**). The significant difference between the calculated radome water-layer loss (0.05 dB) and the measured power transmission losses (maximum of 2.5 dB) is likely because the GPS L1 circularly polarized signals through rain are degraded much more by depolarization than by path attenuation [5] [6]. There was no height or width data available for the rain cell.

Figure 2 shows the measured power transmission loss in dB (blue) and the ex-

ponentially smoothed curve (orange) for GPS satellite PRN 29; the three rain gauge signals are shown by black triangles. As shown in Figure 2, the measured maximum power transmission loss by the light rain is approximately 2.5 dB.

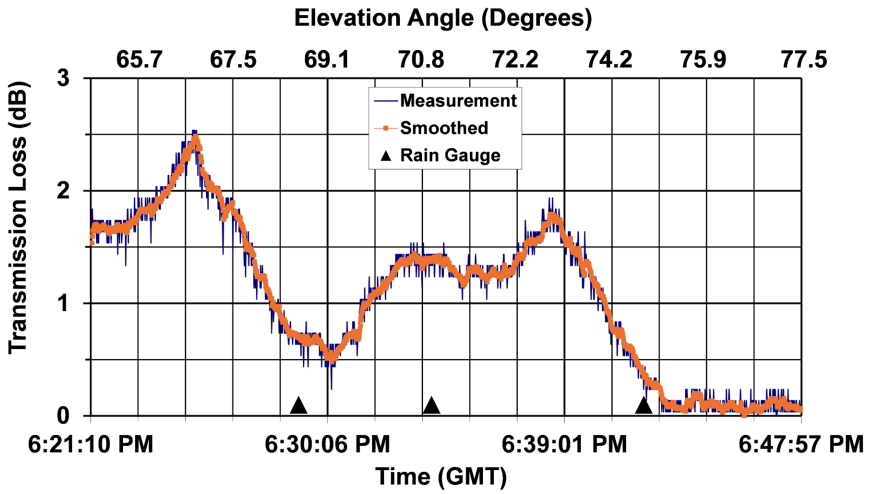

Figure 2. Measured (blue) and smoothed (orange) time plots of power transmission loss for the radome-covered GPS antenna during the light rain (0.75 mm h^{-1}) for GPS satellite PRN 29. The skies were mostly clear from 6:45 p.m. to 6:48 p.m. GMT with a dry radome surface.

The exponential smoothed curve is calculated by Microsoft's Excel Data Analysis Toolpak with a smoothing constant (α) of 0.8. The smoothing formula is

$$P_{t+1} = \alpha P_t + (1-\alpha) P_{t-1} \tag{9}$$

where

P_{t+1}: next power value;

P_{t-1}: previous power value;

P_t: current power value;

α: smoothing constant;

t: discrete time.

Figure 3 shows the measured transmissivity (power transmission) in percent for the light rain event for GPS satellite PRN 29, where the measurements are shown in blue, the exponentially smoothed curve is shown in orange, and the three rain gauge signals are shown by black triangles. The transmittivity (T) in percent is

$$T = \frac{P}{P_{\max}} \times 100 \tag{10}$$

where

$P = 10^{\left(\frac{P_{dB}}{10}\right)}$;

$P_{\max} = 10^{\left(\frac{P_{\max dB}}{10}\right)}$.

Measurements in Figure 3 show that the minimum transmissivity by the light rain is approximately 58%.

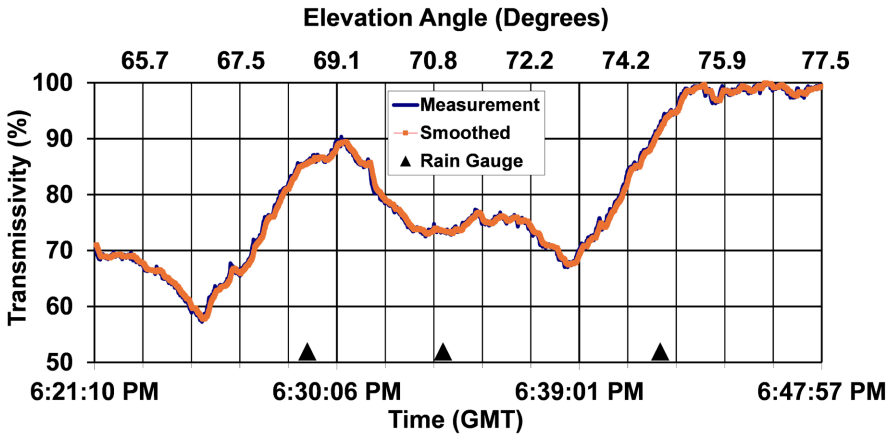

Figure 3. Measured (blue) and smoothed (orange) time plots of transmissivity for the radome-covered GPS antenna during the light rain (0.75 mm h^{-1}) for GPS satellite PRN 29. The skies were mostly clear from 6:45 p.m. to 6:48 p.m. GMT with a dry radome surface.

4. Application of the Results to GPS Signal Degradation by Rain

Tropospheric particles can degrade GPS signals by depolarization and attenuation [6] [23]-[25]. Understanding and quantifying these depolarization and attenuation effects are necessary for optimal GPS use and accuracy. As was shown in Section 3, precipitation in the form of light rain causes GPS signal degradation. Light rain is difficult to model because it is rarely uniform in time and space. Therefore, real-time GPS measurements during light rain would help to quantify these effects. The results from Section 3 show that the GPS power transmission loss through the light rain was variable, with a maximum of approximately 2.5 dB. Therefore, the transmissivity through the light rain was also variable, with a minimum of approximately 58%. However, there are limitations to generalizing about quantifying the depolarization and attenuation effects on GPS signals from a single light rain event with only one GPS satellite. Therefore, future research involving more GPS satellites and rain events is needed to determine the usefulness of this technique.

Furthermore, higher rain rates will degrade GPS signals even more. For example, heavy rain rates of 50 mm h^{-1} and 200 mm h^{-1} (tropical downpour) [4] will produce water-layer thicknesses on the radome of 0.087 and 0.14 mm, respectively, see (1). Therefore, the power transmission losses for these water-layer thicknesses are 0.24 and 0.42 dB, respectively (see Section 2). For a given rain rate, the power transmission loss of the water-layer will be in addition to the power transmission loss of the rain occurring simultaneously on the propagation path [26]. Since the water-layer's power transmission loss is expected to be much less than the rain's power transmission loss on the propagation path, the power transmission loss of the water-layer can be neglected when estimating the power transmission loss of the rain. This technique was used in Section 3 for estimating the power transmission loss of the light rain. This GPS-T technique could potentially improve GNSS-derived perceptible water vapor (PWV) measurements during heavy rainfall events [27] by including the power transmission

loss by raindrops. Although this idea is speculative, it may be worthwhile pursuing its usefulness with future research.

It would be very beneficial if these two loss effects could be separated. However, as Hogg and Chu state [26], "separation of the two effects is a difficult process." Nevertheless, if they could be separated, then the power transmission loss of the rain occurring on the propagation path could be better estimated. Furthermore, with an estimate of the power transmission loss of the water-layer, the rain rate (R) could be calculated as described in Section 2. This would provide a new technique for estimating rain rate. Currently, real-time water-layer thicknesses could be estimated if the rain rate is continuously measured by a device like the capacitor-type rain gauge used in [16]. This would be an improvement over the tipping-bucket-type rain gauge used in this study. An analysis of the real-time water-layer thickness estimates and the continuous rain rate measurements may provide insight into how to estimate the water-layer thickness without an *in situ* rain rate measurement. If this can be accomplished, then it would be a new technique to estimate rain rate compared to the GNSS technique proposed by [28], which uses cross-polarization discrimination (XPD). It should be noted that this proposed XPD technique for estimating rain rate could potentially be improved by placing each receiver antenna under a fiberglass hemispherical radome.

5. Conclusion

GPS is designed to operate in all weather conditions. Quantifying power transmission losses through rain is necessary for optimal GPS use and accuracy. The results presented here provide received power variations of GPS L1 signals caused by light rain for one GPS satellite. Although only one GPS satellite was used in this study, these measurements still show potential for estimating power transmission loss and transmissivity (power transmission) of GPS signals through light rain. Additional measurements for different rain rates and more GPS signals are needed to determine the validity and usefulness of this technique. Future studies will include using more GPS orbital tracks by multiplying the normalized GPS antenna elevation gain pattern with the received GPS signals. Since the normalized GPS antenna azimuth gain pattern is approximately constant, it does not need to be multiplied by the received GPS signals. These additional GPS orbital tracks will improve the spatial or temporal resolution of GPS-T through rain. Furthermore, measurements of each transmitted GPS satellite signal strength during clear sky conditions are needed to quantify the stability of the transmitted signal strength. During the measurements, it was assumed that the transmitted signal strength was constant, see Section 3. This GPS-T technique could potentially improve GNSS-derived PWV measurements during rainfall events by including the power transmission loss by raindrops. Future research will determine if this idea is feasible. Further studies and measurements may lead to a GPS-T technique for inferring rain rate by using a receiving antenna covered by a fiberglass hemispherical radome. Lastly, this GPS-T technique could be expanded for GNSS signals.

The key benefit of such an expansion, by leveraging signals from multiple constellations, is to improve spatial or temporal resolution.

Acknowledgements

The author would like to thank A. Barber of Montana State University Billings, for her critical involvement with this research. This work was supported by the Montana State University Billings Mathematics Department. The author would also like to thank the anonymous reviewers for their very valuable comments and suggestions.

Conflicts of Interest

The author declares no conflicts of interest regarding the publication of this paper.

References

[1] El-Rabbany, A. (2006) Introduction to GPS, The Global Positioning System. 2nd Edition, Artech House.

[2] Bonafoni, S. and Biondi, R. (2016) The Usefulness of the Global Navigation Satellite Systems (GNSS) in the Analysis of Precipitation Events. *Atmospheric Research*, **167**, 15-23. https://doi.org/10.1016/j.atmosres.2015.07.011

[3] Ghosh, A., Farhad, M.M., Hoque, M.E., Boyd, D.R., Bourgeau-Chavez, L., Cosh, M.H., *et al.* (2025) Estimating Vegetation Optical Depth with Mobile GNSS Transmissiometry in Temperate Forests during Smapvex22. *IEEE Journal of Selected Topics in Applied Earth Observations and Remote Sensing*, **18**, 6451-6463. https://doi.org/10.1109/jstars.2025.3541182

[4] Ulaby, F.T., Moore, R.K. and Fung, A.K. (1981) Microwave Remote Sensing, Active and Passive. Vol. I, Addison-Wesley Publishing Company, Inc.

[5] Kobayashi, T. (1976) Pre-Estimation of Cross-Polarization Discrimination Due to Rain. *Journal of the Radio Research Laboratories* (*Japan*), **23**, 47-64. https://ui.adsabs.harvard.edu/abs/1976RaRLJ..23...47K/abstract

[6] Flock, W.L. (1983) Propagation Effects on Satellite Systems at Frequencies below 10 GHz, A Handbook for Satellite Systems Design, NASA, 1108.

[7] Taur, R. (1975) Rain Depolarization Measurements on a Satellite-Earth Propagation Path at 4 GHz. *IEEE Transactions on Antennas and Propagation*, **23**, 854-858. https://doi.org/10.1109/tap.1975.1141200

[8] Hao, A., Wei, Y., Heng, B., Wenjun, L., Yang, F. and Ying, H. (2013) Research on Retrieval of Rain Rate Using Polarimetric GNSS Signals. *Proceedings of the* 2013 *the International Conference on Remote Sensing, Environment and Transportation Engineering* (*RSETE* 2013), Nanjing, 26-28 July 2013, 440-443.

[9] Balasubramaniam, R. and Ruf, C. (2020) Characterization of Rain Impact on L-Band GNSS-R Ocean Surface Measurements. *Remote Sensing of Environment*, **239**, Article 111607. https://doi.org/10.1016/j.rse.2019.111607

[10] Asgarimehr, M., Hoseini, M., Semmling, M., Ramatschi, M., Camps, A., Nahavandchi, H., *et al.* (2022) Remote Sensing of Precipitation Using Reflected GNSS Signals: Response Analysis of Polarimetric Observations. *IEEE Transactions on Geoscience and Remote Sensing*, **60**, 1-12. https://doi.org/10.1109/tgrs.2021.3062492

[11] Asgarimehr, M., Zavorotny, V., Wickert, J. and Reich, S. (2018) Can GNSS Reflec-

tometry Detect Precipitation over Oceans? *Geophysical Research Letters*, **45**, 12585-12592. https://doi.org/10.1029/2018gl079708

[12] Ghavidel, A. and Camps, A. (2016) Impact of Rain, Swell, and Surface Currents on the Electromagnetic Bias in GNSS-Reflectometry. *IEEE Journal of Selected Topics in Applied Earth Observations and Remote Sensing*, **9**, 4643-4649. https://doi.org/10.1109/jstars.2016.2538181

[13] Bansal, R. (1999) The Far Field: How Far Is Far Enough? *Applied Microwave & Wireless*, **11**, 58-60.

[14] Von Hippel, A.R. (1957) Tables of Dielectric Materials. Vol. V, M.I.T. Laboratory for Insulation Research.

[15] Gibble, D. (1964) Effects of Rain on Transmission Performance of a Satellite Communications System. *IEEE International Convention Record*, New York City, 23-26 March 1964, 52.

[16] Anderson, I. (1975) Measurements of 20-GHz Transmission through a Radome in Rain. *IEEE Transactions on Antennas and Propagation*, **23**, 619-622. https://doi.org/10.1109/tap.1975.1141134

[17] Kurri, M. and Huuskonen, A. (2008) Measurements of the Transmission Loss of a Radome at Different Rain Intensities. *Journal of Atmospheric and Oceanic Technology*, **25**, 1590-1599. https://doi.org/10.1175/2008jtecha1056.1

[18] Blevis, B. (1965) Losses Due to Rain on Radomes and Antenna Reflecting Surfaces. *IEEE Transactions on Antennas and Propagation*, **13**, 175-176. https://doi.org/10.1109/tap.1965.1138384

[19] Ulaby, F.T., Moore, R.K. and Fung, A.K. (1986) Microwave Remote Sensing, Active and Passive. Vol. III, Artech House.

[20] Jacobson, M.D. (2010) Snow-Covered Lake Ice in GPS Multipath Reception—Theory and Measurement. *Advances in Space Research*, **46**, 221-227. https://doi.org/10.1016/j.asr.2009.10.013

[21] Jacobson, M.D., Snider, J.B. and Hogg, D.C. (1988) Comparison of Two Multisheet Transmission Windows for Millimeter-Wave Radiometers. *IEEE Transactions on Antennas and Propagation*, **36**, 535-542. https://doi.org/10.1109/8.1143

[22] Gupta, K.C., Garym, R. and Chadha, R. (1981) Computer-Aided Design of Microwave Circuits. Artech House.

[23] Solheim, F.S., Vivekanandan, J., Ware, R.H. and Rocken, C. (1999) Propagation Delays Induced in GPS Signals by Dry Air, Water Vapor, Hydrometeors, and Other Particulates. *Journal of Geophysical Research*: *Atmospheres*, **104**, 9663-9670. https://doi.org/10.1029/1999jd900095

[24] MacGouran, G., Lachapelle, G., Nayak, R. and Wang, A. (2001) Overview of GNSS Signal Degradation Phenomena. *International Symposium on Kinematic Systems in Geodesy*, *Geomatics and Navigation*, Banff, 5-8 June 2001, 87-100. https://www.researchgate.net/publication/242078138_OVERVIEW_OF_GNSS_SIGNAL_DEGRADATION_PHENOMENA

[25] Levis, C.A., Johnson, J.T. and Teixeira, F.L. (2010) Radiowave Propagation: Physics and Applications. John Wiley & Sons, Inc.

[26] Hogg, D.C. and Ta-Shing Chu, (1975) The Role of Rain in Satellite Communications. *Proceedings of the IEEE*, **63**, 1308-1331. https://doi.org/10.1109/proc.1975.9940

[27] Barindelli, S., Realini, E., Venuti, G., Fermi, A. and Gatti, A. (2018) Detection of Water Vapor Time Variations Associated with Heavy Rain in Northern Italy by Geodetic and Low-Cost GNSS Receivers. *Earth, Planets and Space*, **70**, Article No. 28.

https://doi.org/10.1186/s40623-018-0795-7

[28] Yan, W., An, H., Fu, Y., Han, Y., Wang, X. and Ai, W. (2014) A Method for Estimating Rain Rate from Polarimetric GNSS Measurements: Preliminary Analysis. *Atmospheric Research*, **149**, 70-76. https://doi.org/10.1016/j.atmosres.2014.05.016